



# Experimental Study on Strength Properties of MICP-Treated Silty Sand

Mehdi Abbasi <sup>1\*</sup>

<sup>1</sup> Department of Civil Engineering, Faculty of Engineering, University of Guilan, Guilan, Iran.

## Article Info

Received 21 December 2024  
Accepted 12 January 2025  
Available online 06 March 2025

## Keywords:

MICP Treatment;  
Sporosarcina Pasteurii;  
Soil Biological Treatment;  
Unconfined Compressive Strength.

## Abstract:

Microbially induced carbonate precipitation (MICP) using ureolytic bacteria has emerged as a promising technique for geotechnical applications, including soil stabilization, land remediation, and groundwater control. This bio-mediated process relies on urease activity to hydrolyze urea, leading to calcium carbonate precipitation, which enhances soil strength and stiffness. In this study, the mechanical behavior of silica sand treated with MICP was investigated under varying cementation concentrations ( $\mu$ ) (0.25–1 mol/L), cementation ratios ( $\beta$ ) (10–90%), and injection cycles (3, 14, and 21). Key parameters evaluated included unconfined compressive strength (UCS), secant modulus ( $E_{50}$ ), and calcium carbonate content. The results demonstrated a significant correlation between calcite content and mechanical properties, with optimal performance observed at 14.98% calcite content. This configuration yielded a UCS of 1030 kPa and an  $E_{50}$  of 389 MPa, achieved using *Sporosarcina pasteurii*, a  $\beta = 50\%$ , and a  $\mu = 0.75$  mol/L over 21 days. Findings highlight the critical role of injection cycles and cementation concentration in achieving uniform calcium carbonate distribution and enhancing soil behavior. This study underscores the potential of MICP for tailored geotechnical solutions, providing valuable insights into optimizing bio-cementation processes.

© 2025 University of Mazandaran

\*Corresponding Author: mahdiabbasi4312@gmail.com

Supplementary information: Supplementary information for this article is available at <https://cste.journals.umz.ac.ir/>

Please cite this paper as: Abbasi, M. (2025). Experimental Study on Strength Properties of MICP-Treated Silty Sand. Contributions of Science and Technology for Engineering, 1(4), 28-34. doi:10.22080/cste.2025.28436.1010.

## 1. Introduction

Microbially Induced Carbonate Precipitation (MICP) represents a cutting-edge biotechnological approach to soil enhancement. It utilizes the metabolic activity of ureolytic bacteria to precipitate calcium carbonate ( $\text{CaCO}_3$ ) within soil matrices. This biologically driven process offers an eco-friendly alternative to traditional soil stabilization techniques, addressing geotechnical challenges such as improving soil strength, mitigating erosion, and managing groundwater seepage [1].

Several studies have demonstrated that the strength of biocemented soils is significantly influenced by the concentration of the cementation solution (CCS). High CCS yields more significant calcium carbonate precipitation, enhancing soil strength under identical treatment cycles [2–6]. Conversely, research indicates that when calcium carbonate content (CCC) is kept constant, soils treated with lower CCS often exhibit higher strength due to more uniform crystal distribution and enhanced crystal bridging between soil particles [7]. However, using elevated CCS can lead to challenges such as injection point clogging and uneven cementation, potentially reducing specimen uniformity [8–10].

Additionally, the number of treatment cycles plays a pivotal role in determining the performance of MICP-treated soils. Studies have highlighted that increasing the

number of biochemical treatments results in more significant  $\text{CaCO}_3$  deposition, further enhancing unconfined compressive strength (UCS) and other mechanical properties [11]. These findings underscore the complex interactions among CCS, treatment cycles, and calcium carbonate distribution in optimizing the mechanical behavior of bio-cemented soils.

Silica sand, characterized by its poorly graded structure and low natural cohesion, provides an ideal substrate for examining these interactions. This study investigates the effects of varying CCS, cementation ratios, and injection cycles on the mechanical properties of MICP-treated silica sand. By identifying the optimal conditions for maximizing soil performance, this research advances sustainable geotechnical practices and bio-cementation technologies.

## 2. Experimental Approach

### 2.1. Soil Materials

This study utilized silica silty sand sourced from Firoozkooh, northeast of Tehran, Iran. The sand was processed by crushing at the factory, then washing and oven-drying in the laboratory to remove fine particles. The tested sand particles are sub-rounded and exhibit a brown hue, with particle sizes ranging from 0.075 to 2 mm. The maximum dry density of the sand was determined to be 1.95 g/cm<sup>3</sup> in accordance with ASTM D698 [12]. Based on the



particle size distribution curve presented in Figure 1, the sand is classified as SP according to the Unified Soil Classification System (USCS) [13]. The index properties of the Firoozkooh sand and those of the non-cohesive silt are summarized in Table 1.

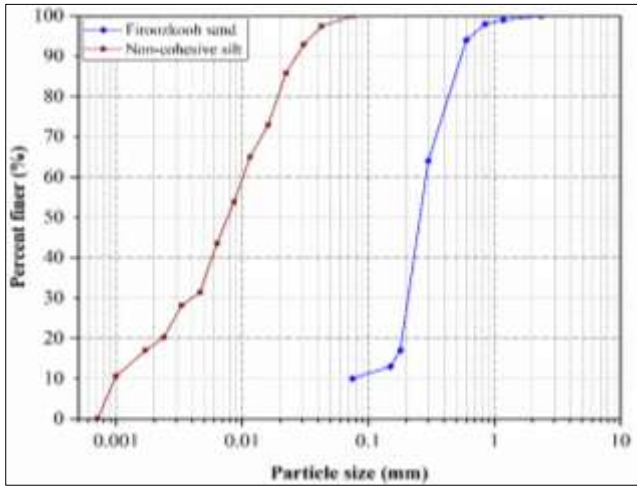


**Figure 1.** Grain size distributions of Firoozkooh sand and non-cohesive silt

**Table 1.** Index properties of Firoozkooh sand and non-cohesive silt used in the experiments

Properties	Firoozkooh sand	Non-cohesive silt
Specific gravity, $G_s$ (-)	2.65	2.66
Maximum dry unit density, $\rho_{d,max}$ ( $g/cm^3$ )	1.98	1.64
Optimum moisture content, $w_{opt}$ (%)	13.11	20.92
Mean grain size, $D_{50}$ (mm)	0.26	0.008
Coefficient of curvature, $C_c$ (-)	2.15	---
Coefficient of uniformity, $C_u$ (-)	3.73	---
Liquid limit, $w_l$ (%)	---	35
Plastic limit, $w_p$ (%)	---	26

## 2.2. Microorganism and Culture Medium

This study obtained the ureolytic bacteria *Sporosarcina pasteurii* from the Persian Type Culture Collection (PTCC 1645). The growth medium preparation followed strict sterilization protocols, with autoclaving carried out at 120°C and 15 psi (103.4 kPa) for 20 minutes [14]. The growth medium consisted of nutrient broth (NB) at a concentration of 25 g/L, providing the essential nutrients required for bacterial proliferation.

After autoclaving, the medium was allowed to cool to room temperature before inoculating it with *S. pasteurii*. To prevent contamination, the inoculation process was conducted under sterile conditions within a laminar airflow cabinet. Post-inoculation, the growth medium was incubated in an orbital shaker at 25°C with a rotation speed of 200 rpm for 24 hours to facilitate bacterial growth. The solution's jars were covered with cotton plugs to ensure aerobic conditions, allowing oxygen exchange while maintaining sterility.

The growth of the bacteria was monitored by measuring the optical density (OD) at a wavelength of 600 nm using a spectrophotometer. The OD600 value was an indicator of bacterial concentration and activity, critical parameters for ensuring consistent bio-cementation efficiency. The prepared bacterial suspension was then utilized for further experimental procedures, ensuring that the OD values were within the optimal range for MICP applications [1].

## 2.3. Sample Preparation

The cylindrical soil specimens, each with a diameter of 45 mm and a height of 90 mm, were reconstructed using a stainless-steel mold. The Firoozkooh silty sand was initially oven-dried at 150°C for 24 hours to eliminate potential contamination from other bacterial species and to facilitate the desired relative compaction ( $R_c$ ) of the soil within the molds [15].

The cementation solution (CS) was pre-cooled to prepare the bacterial stabilizer and then gently mixed with the bacterial suspension to prevent premature calcium carbonate precipitation. This mixture was subsequently combined with the dry, silty sand. The resulting mixture was stored at a low temperature to minimize the risk of unwanted precipitation before placement.

The treated silty sand was then compacted in three layers within the mold to achieve a relative compaction of 90%. The compacted soil was undisturbed for 12 hours at room temperature (25°C) to allow sufficient interaction between the cementation solution and the bacterial suspension. This initial step corresponded to one cycle of MICP treatment.

The cementation solution was injected into the compacted soil specimen to initiate the MICP process. The specimen was then maintained at room temperature for an additional 12 hours to ensure the completion of the reaction between the bacterial solution and the cementation solution [16–18].

## 2.4. Unconfined Compressive Strength (UCS) and Calcite Content Assessment

Unconfined compressive strength (UCS) tests were conducted according to ASTM D2166 [19] for bio-cemented soil samples with a diameter-to-height ratio of 1:2. Axial loads were applied at a constant rate of 1.0 mm/min until specimen failure occurred.

The fractured UCS specimens were subsequently used to determine the calcite content across three layers: upper, middle, and lower regions of the cylindrical samples. Subsamples were collected from the central portions of each layer for analysis. The calcite content was determined using a washing method involving dissolving calcium carbonate in hydrochloric acid. For this procedure, 5 g of the sample was combined with 20 mL of 1-M HCl to dissolve the calcium carbonate. The mixture was then rinsed thoroughly using distilled water on filter paper with coarse pores placed over a No. 200 sieve for 10 minutes. This ensured the removal of all soluble calcium from the sand particles. The solid residue retained on the sieve was oven-dried and weighed. The difference in weight between the initial sand

sample (A) and the washed sample (B) represented the mass of calcium carbonate.

The calcium carbonate content (CCC) was calculated as follows Choi et al. [20]:

$$CCC = \frac{A-B}{A} \times 100 \quad (1)$$

### 3. Results and Discussion

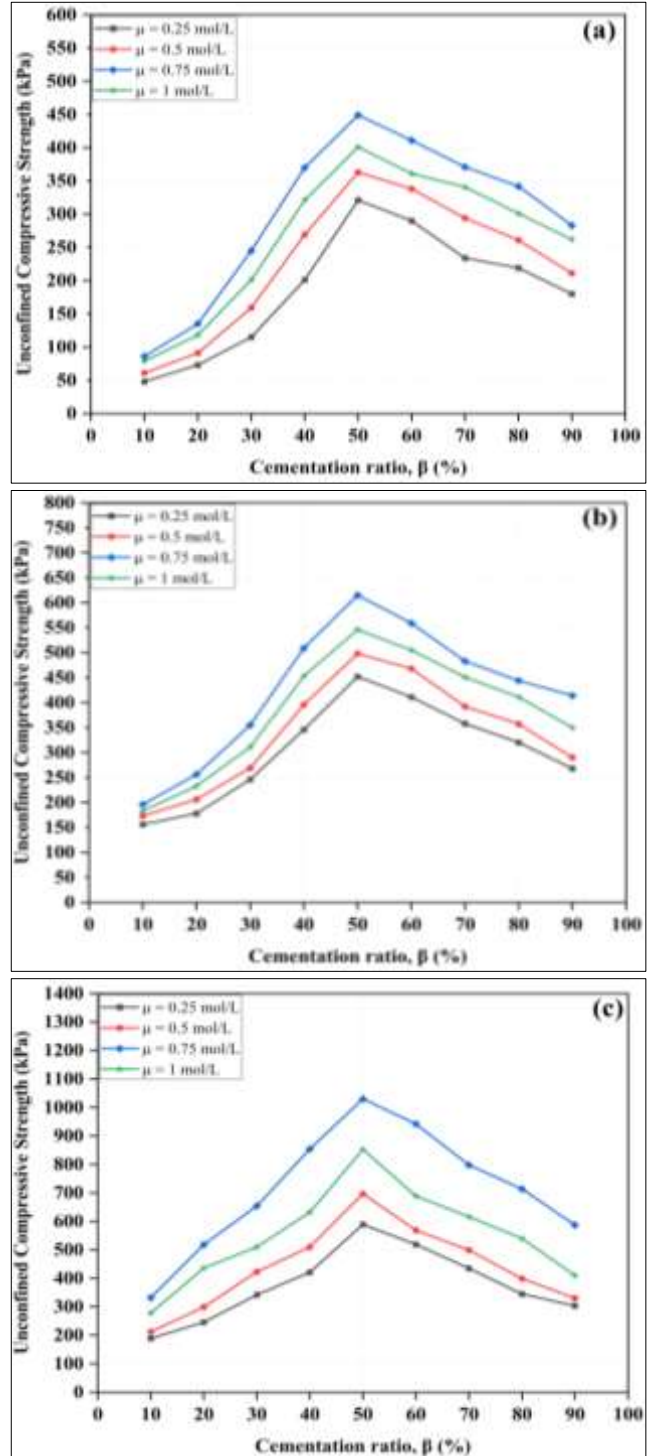
#### 3.1. Effect of Concentration & Content of Cementation Solution

Figure 2 illustrates the UCS values for varying cementation molarity ( $\mu$ ), cementation ratio ( $\beta$ ), and the number of injection cycles. The UCS decreases with lower molarities and cementation ratios, establishing a clear relationship between UCS, cementation solution concentration, and retention time (the interval between successive cementation solution injections) [21]. Adjusting cementation solution concentrations according to retention time achieves comparable bio-cementation efficiency [22]. At  $\beta = 50\%$ , UCS peaks and declines as  $\beta$  increases from 50% to 90%. This trend aligns with the findings of Liu et al. [15] and Sharma et al. [23], who observed that higher  $\beta$  values increase calcium carbonate content, enhancing soil resistance.

Figure 2-a presents UCS values for samples subjected to three injection cycles. When  $\beta$  increased from 10% to 20%, UCS improved by approximately 49%. Further increasing  $\beta$  from 20% to 30% resulted in a 70% increase in UCS, with the maximum UCS recorded at 449 kPa for  $\mu = 0.75$  mol/L. This significant strength enhancement can be attributed to balanced bacterial and cementation solution proportions, facilitating effective calcium carbonate deposition within the soil. Beyond  $\beta = 50\%$ , UCS begins to decline. For instance, UCS decreased by approximately 9% as  $\beta$  increased from 50% to 60% and by 16.75% from  $\beta = 80\%$  to  $\beta = 90\%$ . For all  $\beta$  values, UCS was lowest at  $\mu = 0.25$  mol/L and highest at  $\mu = 0.75$  mol/L, regardless of injection cycles. This can be attributed to the influence of  $\mu$  on calcium carbonate crystal size. Lower  $\mu$  produces smaller crystals, while increasing  $\mu$  results in larger crystals that enhance soil strength through stronger bonding. However, at  $\mu = 1$  mol/L, oversized calcium carbonate crystals caused uneven precipitation, reducing UCS. These findings are consistent with previous studies [24–29].

Figures 2-b and 2-c display UCS values for samples undergoing 14 and 21 injection cycles, respectively. Similar to Figure 2-a, UCS was highest at  $\beta = 50\%$  and decreased as  $\beta$  increased to 90%. Increasing injection cycles strengthened bonds between soil grains, improving resistance. With three cycles, weaker bonds formed. By 14 cycles, crystal growth created bridges between grains, and at 21 cycles, thicker bonds filled gaps, further enhancing strength. These results confirm that increasing injection cycles improves soil resistance, consistent with studies by Mahawish et al. (2019) and Sharma et al. (2021).

Figure 3 presents the variations in  $E_{50}$  derived from uniaxial tests for different cementation molarity ( $\mu$ ), cementation ratio ( $\beta$ ), and the number of injection cycles.



**Figure 2.** UCS vs. concentration and cementation ratio: (a) 3 injection cycles; (b) 14 injection cycles; (c) 21 injection cycles

Figure 3-a shows the  $E_{50}$  values for samples subjected to 3 injection cycles. At  $\beta = 10\%$ ,  $E_{50}$  values are relatively consistent across all  $\mu$  levels, ranging between 10 and 20 MPa. As  $\beta$  increases to 20%,  $E_{50}$  improves significantly, particularly at higher  $\mu$  levels (0.75 mol/L and 1 mol/L), where  $E_{50}$  reaches approximately 35 MPa. The improvement is modest for lower  $\mu$  levels (0.25 mol/L and 0.5 mol/L), yielding  $E_{50}$  values around 20 MPa. Interestingly, at  $\beta = 10\%$ , 20%, and 90%,  $E_{50}$  values for  $\mu = 0.75$  mol/L and  $\mu = 1$  mol/L are nearly identical, indicating similar behavior at these  $\beta$  levels.



The maximum  $E_{50}$  is observed at  $\beta = 50\%$ , with values increasing from 100 MPa to 140 MPa across various  $\mu$  levels. However, as  $\beta$  rises from 50% to 90%,  $E_{50}$  gradually decreases, though the reduction rate is modest, resulting in a shallow slope on the graph. For instance, at  $\beta = 60\%$ ,  $E_{50}$  varies between 96 MPa and 133 MPa, reflecting a minor decrease compared to  $\beta = 50\%$ . Regarding the effect of  $\mu$  on  $E_{50}$ , at  $\beta = 10\%$ ,  $E_{50}$  ranges from 11.5 MPa to 21.5 MPa, showing an 87% increase between  $\mu = 0.25$  mol/L and  $\mu = 0.75$  mol/L. At  $\beta = 50\%$ , the increase is approximately 41.5%. Across all  $\beta$  values, specimens with  $\mu = 0.25$  mol/L consistently show the lowest  $E_{50}$ , while those with  $\mu = 0.75$  mol/L demonstrate the highest values.

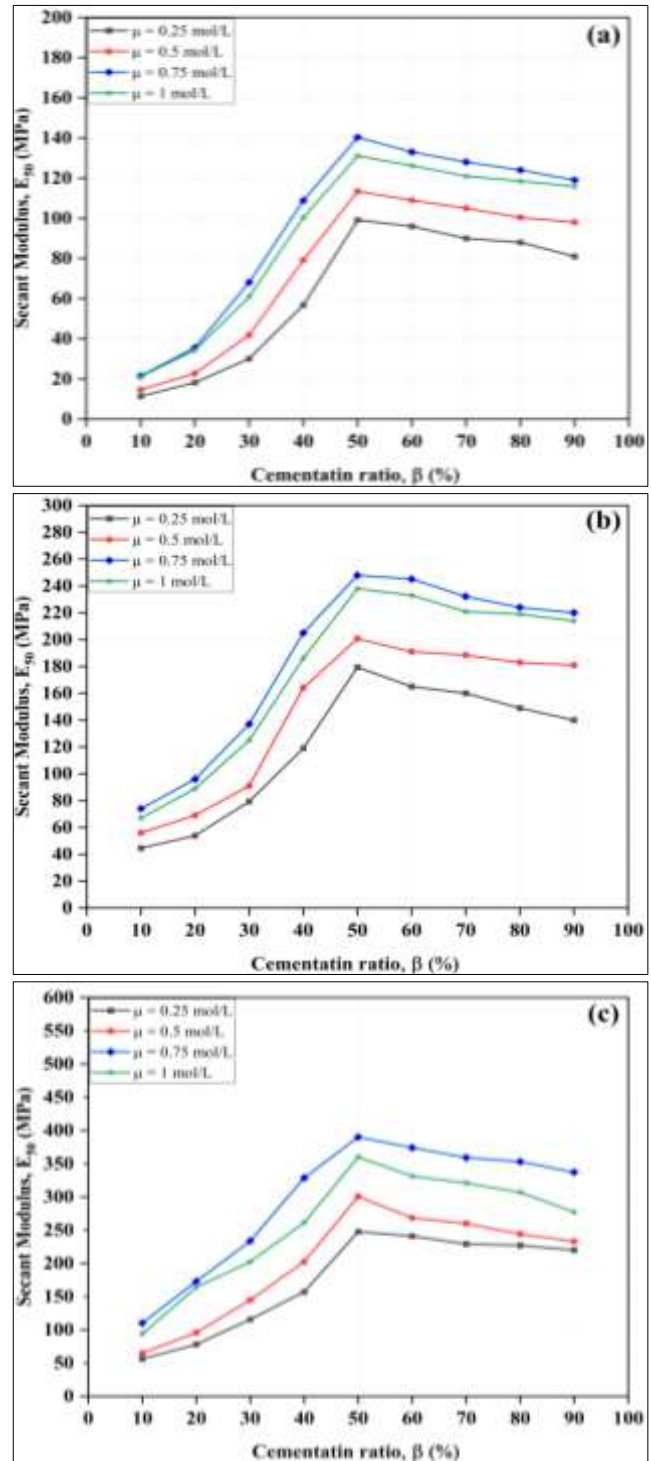
Figure 3-b illustrates  $E_{50}$  values for samples subjected to 14 injection cycles. Similar to the results for 3 cycles, the highest  $E_{50}$  is observed at  $\beta = 50\%$ , with values reaching up to 248 MPa for different  $\mu$  levels. As  $\beta$  increases from 50% to 90%,  $E_{50}$  decreases gradually, with a slower reduction rate than the 3-cycle results. The  $\mu = 0.25$  mol/L samples exhibit the lowest  $E_{50}$ , while  $\mu = 0.5$  mol/L samples display higher values than those with  $\mu = 0.25$  mol/L. A notable difference between 14-cycle and 3-cycle results is the increasing disparity in  $E_{50}$  between  $\mu = 0.25$  mol/L and  $\mu = 0.5$  mol/L as  $\beta$  rises from 60% to 90%. However, the difference in  $E_{50}$  between  $\mu = 0.75$  mol/L and  $\mu = 1$  mol/L remains nearly constant, regardless of the number of injection cycles.

Figure 3-c depicts  $E_{50}$  values for samples treated with 21 injection cycles. As with the previous injection cycles, the highest  $E_{50}$  is observed at  $\beta = 50\%$ , reaching values up to 390 MPa for different  $\mu$  levels. As  $\beta$  increases from 50% to 90%,  $E_{50}$  decreases gradually, following trends in 3-cycle and 14-cycle results. In 21-cycle tests,  $\mu = 0.25$  mol/L yields the lowest  $E_{50}$  values again, while  $\mu = 0.5$  mol/L produces higher values than  $\mu = 0.25$  mol/L. However, unlike the 14-cycle results, the difference in  $E_{50}$  between  $\mu = 0.25$  mol/L and  $\mu = 0.5$  mol/L diminishes as  $\beta$  rises from 60% to 90%. Conversely, the gap in  $E_{50}$  between  $\mu = 0.75$  mol/L and  $\mu = 1$  mol/L becomes more pronounced compared to 3-cycle and 14-cycle results. The results suggest that increasing  $\beta$  enhances cementation solution content, resulting in more brittle behavior and increased stiffness in treated samples. Higher  $\mu$  values generally lead to increased stiffness. However, at  $\mu = 1$  mol/L, the crystal sizes exceed particle spacing, causing uneven calcium carbonate precipitation, which reduces sample hardness compared to  $\mu = 0.75$  mol/L.

### 3.2. Calcite Content Assessment

The calcite content strongly correlates with UCS and  $E_{50}$ . Figure 4 highlights the interplay between these parameters and calcite content percentages. In this study, samples with varying molarities ( $\mu = 0.25, 0.5, 0.75,$  and  $1$  mol/L) and different numbers of injection cycles (3, 14, and 21) under a constant  $\beta = 50\%$  were analyzed to assess the impact of calcite content on UCS and  $E_{50}$ . Figure 4-a illustrates UCS variations as a function of calcite content, considering the combined effects of  $\mu$ , injection cycles, and a consistent  $\beta = 50\%$ . The sample with  $\mu = 0.25$  mol/L subjected to 3 injection cycles exhibited the lowest UCS and calcite

content. UCS and calcite content improved by increasing the number of injection cycles to 14 for the same molarity (0.25 mol/L). For example, the sample treated with 14 cycles achieved a UCS of 450 MPa with a calcite content of 7.14%. Increasing the number of injection cycles from 14 to 21 further enhanced both UCS and calcite content, a trend consistent across all molarities. This underscores the role of injection cycles in increasing strength and calcite deposition.



**Figure 3.**  $E_{50}$  vs. concentration and cementation ratio: (a) 3 injection cycles; (b) 14 injection cycles; (c) 21 injection cycles

Additionally, elevating the molarity from  $\mu = 0.25$  mol/L to  $\mu = 0.5$  mol/L led to greater UCS and calcite content

within each cycle, demonstrating the influence of molarity on these properties. While higher molarities corresponded to more significant calcite deposition, samples with  $\mu = 0.75$  mol/L consistently exhibited the highest UCS. Thus, although calcite content increased with more cycles, the peak UCS was achieved at  $\mu = 0.75$  mol/L. The increase in calcite proportion is attributed to the higher concentration of substrates introduced into the coarse sand pores during successive biochemical treatment cycles. A single bacterial suspension cycle was insufficient to produce significant calcium carbonate precipitation, as noted by Mahawish et al. [30].

Figure 4-b depicts changes in  $E_{50}$  concerning calcite content, considering molarity, injection cycles, and a consistent  $\beta = 50\%$ . Consistent with earlier findings, UCS and  $E_{50}$  are directly correlated. As evident from Figure 4-b, increasing injection cycles and molarity ( $\mu$ ) enhances calcite content. However, samples with  $\mu = 0.25$  mol/L per cycle exhibited the lowest  $E_{50}$ , while those with  $\mu = 0.75$  mol/L per cycle showed the highest values.

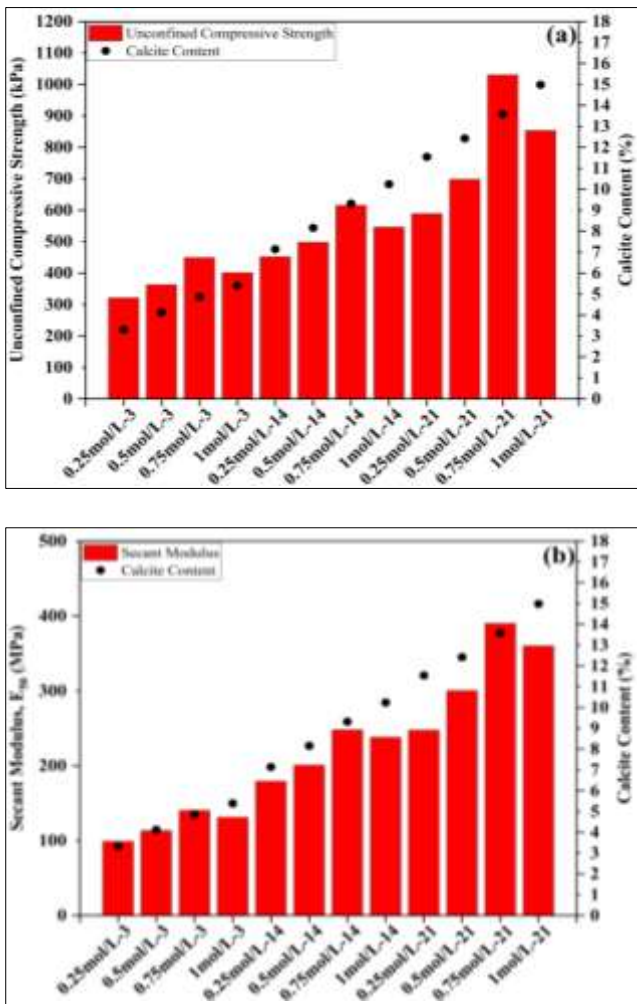


Figure 4. Influence of calcite content, molarity, and injection cycles on: (a) UCS; (b)  $E_{50}$

When a substantial number of biochemical treatment cycles (21 cycles) were applied, calcite crystals with irregular shapes were observed. These irregularities may result from the overlay of thin calcite flakes, which typically

exhibit trigonal to rhombohedral forms. The calcium carbonate formed after extensive treatments can be classified as calcite based on its morphology [31]. Additionally, spherical calcium carbonate crystals were microscopically observed in coarse sand samples treated with four biochemical cycles, as reported by Mahawish et al. [30].

#### 4. Conclusion

A comprehensive set of unconfined compressive strength (UCS) tests was conducted to evaluate the strength and stiffness of silty sand specimens treated using the microbially induced calcium carbonate precipitation (MICP) method. The effects of molarity, cementation ratio, and injection cycles were simultaneously investigated. The key findings of the study are summarized as follows:

The UCS and secant modulus ( $E_{50}$ ) were significantly influenced by the molarity of cementation materials. For specimens subjected to 21 injection cycles, increasing the molarity from 0.25 to 0.75 mol/L increased approximately 74.8% in UCS and 57.5% in  $E_{50}$ . However, further increasing the molarity to 1 mol/L caused reductions of about 17.1% in UCS and 7.7% in  $E_{50}$ . This trend suggests that at  $\mu = 0.75$  mol/L, the size of the formed calcium carbonate crystals closely matches the pore size of soil grains, achieving optimal precipitation and maximum UCS and  $E_{50}$  values. At  $\mu = 1$  mol/L, the bond length increases, leading to uneven calcium carbonate distribution, negatively impacting strength and stiffness.

Increasing the cementation ratio from 10% to 50% led to substantial improvements in UCS and  $E_{50}$ , with maximum calcium carbonate precipitation observed at  $\beta = 50\%$ . However, increasing the cementation ratio to 90% significantly reduced these properties. This decline is attributed to decreased calcium carbonate precipitation at higher cementation ratios, adversely affecting strength and stiffness.

An increase in injection cycles from 3 to 21 significantly enhanced calcium carbonate precipitation. This improvement contributed to higher UCS and  $E_{50}$  values due to the forming of more substantial and thicker bonds between soil grains. The increased number of injection cycles allowed more robust crystal development, resulting in greater soil strength and stiffness.

#### 5. References

- [1] Abbasi, M., Hosseinpour, I., Barari, A., & Mirmoradi, S. H. (2025). Mechanical Properties of Silty Sand Treated with MICP Technique Subjected to Freeze-Thaw Cycles. *Transportation Infrastructure Geotechnology*, 12(1), 34. doi:10.1007/s40515-024-00468-6.
- [2] Zhang, X., Wang, H., Wang, Y., Wang, J., Cao, J., & Zhang, G. (2024). Improved methods, properties, applications and prospects of microbial induced carbonate precipitation (MICP) treated soil: A review. *Biogeotechnics*, 100123. doi:10.1016/j.bgtech.2024.100123.

- [3] Li, G., Zhang, Y. J., Hua, X. Q., Liu, J., & Liu, X. (2024). Mechanical properties of aeolian sand cemented via microbially induced calcite precipitation (MICP). *Scientific Reports*, 14(1), 22745. doi:10.1038/s41598-024-73986-5.
- [4] Zhu, T., He, R., Hosseini, S. M. J., He, S., Cheng, L., Guo, Y., & Guo, Z. (2024). Influence of precast microbial reinforcement on lateral responses of monopiles. *Ocean Engineering*, 307, 119493. doi:10.1016/j.oceaneng.2024.118211.
- [5] Wang, Z., Li, Y., Bai, L., Hou, C., Zheng, C., & Li, W. (2025). Biodegradation of polypropylene microplastics by *Bacillus pasteurii* isolated from a gold mine tailing. *Emerging Contaminants*, 11(1), 100397. doi:10.1016/j.emcon.2024.100397.
- [6] Yin, J., Qu, W., Yibulayimu, Z., & Qu, J. (2024). Enhancing aeolian sand stability using microbially induced calcite precipitation technology. *Scientific Reports*, 14(1), 23876. doi:10.1038/s41598-024-74170-5.
- [7] Lai, H. J., Cui, M. J., Wu, S. F., Yang, Y., & Chu, J. (2021). Retarding effect of concentration of cementation solution on biocementation of soil. *Acta Geotechnica*, 16(5), 1457–1472. doi:10.1007/s11440-021-01149-1.
- [8] Wang, Y., Chang, X., Zhang, G., Zeng, Z., Huang, X., Wang, M., & Ma, M. (2024). Pore structure of the mixed sedimentary reservoir of Permian Fengcheng Formation in the Hashan area, Junggar Basin. *Scientific Reports*, 14(1), 1–21. doi:10.1038/s41598-024-71646-2.
- [9] Ge, J., Zhao, W., Wang, S., Hu, S., & Chen, G. (2024). Study on the fluidity of the pore-fracture binary system in a tight sandstone reservoir-NMR. *Geomechanics and Geophysics for Geo-Energy and Geo-Resources*, 10(1). doi:10.1007/s40948-024-00810-9.
- [10] Gadhvi, M. S., Javia, B. M., Vyas, S. J., Patel, R., & Dudhagara, D. R. (2024). *Bhargavaea beijingensis* a promising tool for bio-cementation, soil improvement, and mercury removal. *Scientific Reports*, 14(1), 23976. doi:10.1038/s41598-024-75019-7.
- [11] Mujah, D., Cheng, L., & Shahin, M. A. (2019). Microstructural and Geomechanical Study on Biocemented Sand for Optimization of MICP Process. *Journal of Materials in Civil Engineering*, 31(4). doi:10.1061/(asce)mt.1943-5533.0002660.
- [12] ASTM D698-12(2021). (2021). Standard Test Methods for Laboratory Compaction Characteristics of Soil Using Standard Effort (12,400 ft-lbf/ft<sup>3</sup> (600 kN-m/m<sup>3</sup>)). ASTM International, Pennsylvania, United States. doi:10.1520/D0698-12R21.
- [13] ASTM D2487-17. (2020). Standard Practice for Classification of Soils for Engineering Purposes (Unified Soil Classification System). ASTM International, Pennsylvania, United States. doi 10.1520/D2487-17.
- [14] Dagliya, M., Satyam, N., Sharma, M., & Garg, A. (2022). Experimental study on mitigating wind erosion of calcareous desert sand using spray method for microbially induced calcium carbonate precipitation. *Journal of Rock Mechanics and Geotechnical Engineering*, 14(5), 1556–1567. doi:10.1016/j.jrmge.2021.12.008.
- [15] [Liu, L., Liu, H., Stuedlein, A. W., Evans, T. M., & Xiao, Y. (2019). Strength, stiffness, and microstructure characteristics of biocemented calcareous sand. *Canadian Geotechnical Journal*, 56(10), 1502–1513. doi:10.1139/cgj-2018-0007.
- [16] Mitchell, J. K., & Santamarina, J. C. (2005). Biological Considerations in Geotechnical Engineering. *Journal of Geotechnical and Geoenvironmental Engineering*, 131(10), 1222–1233. doi:10.1061/(asce)1090-0241(2005)131:10(1222).
- [17] Chowdhury, R., Flentje, P., Bhattacharya, G. (2013). *Geotechnics in the Twenty-First Century, Uncertainties and Other Challenges: With Particular Reference to Landslide Hazard and Risk Assessment. Proceedings of the International Symposium on Engineering under Uncertainty: Safety Assessment and Management (ISEUSAM - 2012)*. Springer, India. doi:10.1007/978-81-322-0757-3\_2.
- [18] Chu, J., Stabnikov, V., & Ivanov, V. (2012). Microbially Induced Calcium Carbonate Precipitation on Surface or in the Bulk of Soil. *Geomicrobiology Journal*, 29(6), 544–549. doi:10.1080/01490451.2011.592929.
- [19] ASTM D2166-06. (2010). Standard Test Method for Unconfined Compressive Strength of Cohesive Soil. ASTM International, Pennsylvania, United States doi:10.1520/D2166-06
- [20] Choi, S.-G., Park, S.-S., Wu, S., & Chu, J. (2017). Methods for Calcium Carbonate Content Measurement of Biocemented Soils. *Journal of Materials in Civil Engineering*, 29(11). doi:10.1061/(asce)mt.1943-5533.0002064.
- [21] Zeitouny, J., Lieske, W., Alimardani Lavasan, A., Heinz, E., Wichern, M., & Wichtmann, T. (2023). Impact of New Combined Treatment Method on the Mechanical Properties and Microstructure of MICP-Improved Sand. *Geotechnics*, 3(3), 661–685. doi:10.3390/geotechnics3030036.
- [22] Al Qabany, A., Soga, K., & Santamarina, C. (2012). Factors Affecting Efficiency of Microbially Induced Calcite Precipitation. *Journal of Geotechnical and Geoenvironmental Engineering*, 138(8), 992–1001. doi:10.1061/(asce)gt.1943-5606.0000666.
- [23] Sharma, M., Satyam, N., & Reddy, K. R. (2021). Effect of freeze-thaw cycles on engineering properties of biocemented sand under different treatment conditions. *Engineering Geology*, 284, 106022. doi:10.1016/j.enggeo.2021.106022.
- [24] Cui, M. J., Zheng, J. J., Zhang, R. J., Lai, H. J., & Zhang, J. (2017). Influence of cementation level on the strength behaviour of bio-cemented sand. *Acta Geotechnica*, 12(5), 971–986. doi:10.1007/s11440-017-0574-9.

- [25] Sharma, M., & Satyam, N. (2021). Strength and durability of biocemented sands: Wetting-drying cycles, ageing effects, and liquefaction resistance. *Geoderma*, 402, 115359. doi:10.1016/j.geoderma.2021.115359.
- [26] Chang, Z., Long, G., Xie, Y., & Zhou, J. L. (2022). Recycling sewage sludge ash and limestone for sustainable cementitious material production. *Journal of Building Engineering*, 49, 104035. doi:10.1016/j.jobbe.2022.104035.
- [27] Ahenkorah, I., Rahman, M. M., Karim, M. R., & Beecham, S. (2023). Unconfined compressive strength of MICP and EICP treated sands subjected to cycles of wetting-drying, freezing-thawing and elevated temperature: Experimental and EPR modelling. *Journal of Rock Mechanics and Geotechnical Engineering*, 15(5), 1226–1247. doi:10.1016/j.jrmge.2022.08.007.
- [28] Wen, K., Li, Y., Liu, S., Bu, C., & Li, L. (2019). Development of an Improved Immersing Method to Enhance Microbial Induced Calcite Precipitation Treated Sandy Soil through Multiple Treatments in Low Cementation Media Concentration. *Geotechnical and Geological Engineering*, 37(2), 1015–1027. doi:10.1007/s10706-018-0669-6.
- [29] Ahenkorah, I., Rahman, M. M., Karim, M. R., & Beecham, S. (2023). Characteristics of MICP and EICP-Treated sands in simple shear conditions: A benchmarking with the critical state of untreated sand. *Geotechnique*. doi:10.1680/jgeot.22.00329.
- [30] Mahawish, A., Bouazza, A., & Gates, W. P. (2019). Factors affecting the bio-cementing process of coarse sand. *Proceedings of the Institution of Civil Engineers: Ground Improvement*, 172(1), 25–36. doi:10.1680/jgrim.17.00039.
- [31] Zhao, Q., Li, L., Li, C., Li, M., Amini, F., & Zhang, H. (2014). Factors Affecting Improvement of Engineering Properties of MICP-Treated Soil Catalyzed by Bacteria and Urease. *Journal of Materials in Civil Engineering*, 26(12). doi:10.1061/(asce)mt.1943-5533.0001013.